RESTORATION OF ERROR-DIFFUSED IMAGES USING POCS

Gözde Bozkurt

Dept of Electrical and Computer Engineering
North Carolina State University, Raleigh, NC

A. Enis Çetin

Dept of Electrical Engineering
Bilkent University, Ankara, Turkey

ABSTRACT

Halftoning is a process that deliberately injects noise into the original image in order to obtain visually pleasing output images with a smaller number of bits per pixel for displaying or printing purposes. In this paper, a novel inverse halftoning method is proposed to restore a continuous tone image from the given halftone image. A set theoretic formulation is used where three sets are defined using the prior information about the problem. A new space domain projection is introduced assuming the halftoning is performed with error diffusion, and the error diffusion filter kernel is known. The space domain, frequency domain, and space-scale domain projections are used alternately to obtain a feasible solution for the inverse halftoning problem which does not have a unique solution.

1. INTRODUCTION

Halftoning refers to the problem of rendering continuous-tone (contone) images on display and printing devices which are capable of reproducing only a limited number of colors. Halftoning techniques are used to overcome the contouring problem encountered when direct quantization is applied. Widely used halftoning technique is the error diffusion which works by distributing the previous quantization errors to neighboring pixels. Inverse halftoning is the problem of recovering a contone image from a given halftone image. Contone images are needed in many practical applications. However, inverse halftoning problem is ill-posed because halftoning is a many-to-one mapping, and does not a have a unique solution [1]. Therefore, incorporation of all available information significantly improves the quality of the solution. Our work is motivated by the fact that set theoretic formulation is ideally suitable for the inverse halftoning problem that has many feasible solutions.

The previous inverse halftoning methods employ space-domain operations, frequency-domain operations, or both, or only space-scale domain operations. The simplest approach is lowpass filtering the halftone image to remove the high-frequency components where the halftoning noise is mostly concentrated. Different lowpass filters have been used such as halfband lowpass in [1], Gaussian lowpass and lowpass filtering based on singular value decomposition (SVD) [2]. However, lowpass filtering alone does not work well since this also destroys high-frequency information of the original image.

A projection algorithm, which is essentially an error diffusion with an additional inverse quantization step is proposed in [1], using a maximum a posteriori probability (MAP) projection. A similar method [3], based on a MAP estimator is proposed where a constrained optimization is solved using iterative techniques.

Xiong, Orchard, and Ramchandran [5] proposed an inverse halftoning scheme using wavelets. The idea behind the wavelet decomposition of a halftone image is to selectively choose useful information from each subband. This approach can be considered as a space-scale domain method. No a priori knowledge about the halftoning process is assumed.

The method of Projection Onto Convex Sets (POCS) is used in [4, 2] where information known about the problem is expressed in the form of two constraint sets. In [2, 4], the halftoning process is assumed to be known a priori. Based on this information and the smoothness of most natural images convex sets are defined. The iterative restoration algorithm is developed by making successive projections onto the convex sets. The first set is the set of all contone images when halftoned produce the halftone image that we have, and the second is the set of all images bandlimited to a certain low-pass band. The computational cost of the space-domain projection in [2] turns out to be very high.

In this paper, a new inverse halftoning method based on the method POCS is proposed. Space, frequency, and space-scale (or wavelet) domain projections are used which take advantage of the prior knowledge about the error diffusion filter kernel, and the relatively smooth character of the natural images. The simulation results are presented, and it is experimentally observed that higher quality images can be obtained compared to [2, 1, 5].

2. A SET THEORETIC INVERSE HALFTONING

In our inverse halftoning algorithm, we define three kinds of sets describing the prior information that we have. The set $\boldsymbol{C}_{1,s}$ contains all contone images that result in an observed error diffused pixel at the index s. The set $\boldsymbol{C}_1 = \bigcap_s \boldsymbol{C}_{1,s}$ is the set of all contone images $\boldsymbol{x}$ producing the observed error diffused image $\boldsymbol{y}$. The set $\boldsymbol{C}_2$ contains all band-limited contone images. Finally, the set $\boldsymbol{C}_3$ contains all the images having the same significant Wavelet Transform (WT) local extrema as the original image. These sets are shown to be convex in [6].

The POCS based iterative algorithm starts with an initial estimate $\boldsymbol{x}_0$, which is successively projected onto the sets $\boldsymbol{C}_{1,s}$, $\boldsymbol{C}_2$ and $\boldsymbol{C}_3$, as follows

$$\boldsymbol{x}_{\ell+1} = (P_{1,0} \circ \ \ldots \ \circ P_{1,L} \circ P_2 \circ P_3)\boldsymbol{x}_\ell, \qquad \ell = 0, 1, 2, ...$$

where $P_{1,s}$ represents the spatial projection which will be described in the next subsection, (L is the total number of pixels in the image), P_2 represents lowpass filtering which is the frequency-domain projection, and P_3 represents the wavelet-domain space-scale projection which can be implemented using the algorithm described in [10]. All three projections, or any two can be used alternately. The algorithm is globally convergent to a solution which is in the intersection of all the convex sets regardless of the initial estimate, and the order of the projections is immaterial [7]. The

iterations are stopped when the difference between the signals at successive iterations become insignificant.

2.1. A New Space-domain Projection

The block diagram of error diffusion encoder is given in Figure 1. The inverse halftoning problem can be stated as follows: Given the halftoned image $\boldsymbol{y}$ and the 2-D FIR error diffusion filter kernel $\boldsymbol{h}$, we want to estimate the original image $\boldsymbol{x}$. The variable $\boldsymbol{u}$, which is the input to the quantizer plays a significant role because the uniform quantization operator $\boldsymbol{Q}$ determines the bounds on $\boldsymbol{u}$ for each output pixel $\boldsymbol{y}(s)$.

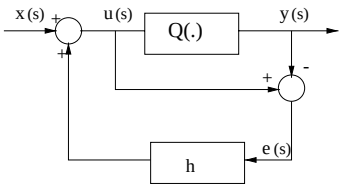

Figure 1: Block diagram of error diffusion method.

Writing the equations for the error diffusion system in Figure 1, we get,

$$\begin{aligned} \boldsymbol{e} &= \boldsymbol{u} - \boldsymbol{y} && (1)\\ \boldsymbol{u} &= \boldsymbol{x} + \boldsymbol{h} * \boldsymbol{e} && (2)\\ (\boldsymbol{I} - \boldsymbol{h}) * \boldsymbol{u} &= \boldsymbol{x} - \boldsymbol{h} * \boldsymbol{y}. && (3) \end{aligned}$$

The image $\boldsymbol{u}$ can be expressed in terms of images $\boldsymbol{x}$ and $\boldsymbol{y}$ as

$$\boldsymbol{u} = (\boldsymbol{I} - \boldsymbol{h})^{-1} * [\boldsymbol{x} - \boldsymbol{h} * \boldsymbol{y}]. \quad (4)$$

Here $*$ denotes the convolution operation, and $\boldsymbol{x}$ is the estimate obtained at each iteration. The kernels for the FIR filters $\boldsymbol{h}$ and $\boldsymbol{I} - \boldsymbol{h}$ are given in Figure 2.

0	0	7/16
3/16	5/16	1/16

h

0	1	-7/16
-3/16	-5/16	-1/16

I-h

Figure 2: Kernels for the filters $\boldsymbol{h}$ and $\boldsymbol{I} - \boldsymbol{h}$.

For convenience, we define

$$\bar{\boldsymbol{x}} = \boldsymbol{x} - \boldsymbol{h} * \boldsymbol{y}. \quad (5)$$

The 2-D IIR inverse filter $\boldsymbol{w} = (\boldsymbol{I} - \boldsymbol{h})^{-1}$ can be approximated by a 2-D FIR filter using a method described in [8] for inverse filtering for image restoration. The size of the filter $\boldsymbol{w}$ is chosen as $m_1 \times m_2$ ($= 50 \times 51$ in our simulations).

The pixel $\boldsymbol{u}(s) = (\boldsymbol{w} * \bar{\boldsymbol{x}})(s)$ can be represented as $\boldsymbol{u}(s) = \sum_{k \in F_v} \boldsymbol{v}(k,s)\, \bar{\boldsymbol{x}}(k)$, where $\boldsymbol{v}$ is the mask corresponding to the filter $\boldsymbol{w}$, and F_v is the support of the mask $\boldsymbol{v}$. For convenience, 1-D indexing is used, although the blocks $\bar{\boldsymbol{x}}$ in F_v, and the mask $\boldsymbol{v}$ are 2-D signals. We use the information at our hand to form a constraint on the image $\bar{\boldsymbol{x}}$ as follows:

$$\begin{aligned} &\text{if } (\boldsymbol{y}(s) = 0 \text{ and } \boldsymbol{u}(s) \geq \delta_q) \text{ or } (\boldsymbol{y}(s) = 255 \text{ and } \boldsymbol{u}(s) < \delta_q)\\ &\quad \text{then } \sum_{k \in F_v} \boldsymbol{v}(k,s)\, \bar{\boldsymbol{x}}(k) = \delta_q \end{aligned} \quad (6)$$

where δ_q is 128 in the case of the binary quantizer. Equation (6) is a hyper-plane, therefore it is a convex set.

The projection onto the set $\boldsymbol{C}_{1,s}$ can be carried out as follows. Let $\bar{\boldsymbol{x}}_p$ be the current iterate. The next iterate $\bar{\boldsymbol{x}}_{p+1}$ is obtained by solving the optimization problem:

$$\min \ \| \bar{\boldsymbol{x}}_{p+1} - \bar{\boldsymbol{x}}_p \|^2 \quad \text{subject to} \quad (6). \quad (7)$$

Using Lagrange multipliers method for this constrained minimization problem, we write

$$\mathcal{L} = \| \bar{\boldsymbol{x}}_{p+1} - \bar{\boldsymbol{x}}_p \|^2 + \mu \Big(\sum_{k \in F_v} \boldsymbol{v}(k,s) \bar{\boldsymbol{x}}_{p+1}(k) - \delta_q \Big). \quad (8)$$

Equating partial derivatives of $\mathcal{L}$ with respect to $\bar{\boldsymbol{x}}_{p+1}$ and μ to 0, and rearranging them gives the projection operation

$$\bar{\boldsymbol{x}}_{p+1} = \bar{\boldsymbol{x}}_p + \lambda \left(\frac{\delta_q - \sum_k \boldsymbol{v}(k,s) \bar{\boldsymbol{x}}_p(k)}{\sum_k \boldsymbol{v}(k,s)^2} \right) \boldsymbol{v} \quad (9)$$

where λ is a relaxation parameter and if it remains between 0 and 2, the convergence of the POCS procedure is assured [7].

The projection given in (9) is performed pixel by pixel involving the block defined by the causal mask $\boldsymbol{v}$ in the image $\bar{\boldsymbol{x}}$. Block size is equal to the support size of the inverse filter $\boldsymbol{w}$. Once we obtain the corrected image $\bar{\boldsymbol{x}}$, we get the new estimate $\boldsymbol{x}$ from (5).

This scheme can be easily extended to the case of multi-level error-diffusion in which the quantizer is not binary. In this case, the image $\boldsymbol{u}$ is quantized to K gray levels by error-diffusion coding, and we want to obtain full gray-scale image. Here,

$$\begin{array}{ccccc} \boldsymbol{A}(s) & \leq & \mathbf{u}(s) & \leq & \boldsymbol{B}(s) \\ \boldsymbol{A}(s) & \leq & \sum_{k \in F_v} \boldsymbol{v}(k,s) \bar{\boldsymbol{x}}(k) & \leq & \boldsymbol{B}(s) \end{array} \quad (10)$$

where the matrices $\boldsymbol{A}$ and $\boldsymbol{B}$ define the quantizer bounds corresponding to the sample $\boldsymbol{u}(s)$. For the binary quantizer, $\boldsymbol{A}(s) = \boldsymbol{u}_{low}(s) = 0$, and $\boldsymbol{B}(s) = \boldsymbol{u}_{high}(s) = 128 - \epsilon$ for the output 0, and $\boldsymbol{A}(s) = \boldsymbol{u}_{low}(s) = 128$, and $\boldsymbol{B}(s) = \boldsymbol{u}_{high}(s) = 255$ for the output 255. For a multi-level uniform quantizer, $\boldsymbol{u}_{low}(s)$ and $\boldsymbol{u}_{high}(s)$ are determined according to the quantizer bounds. If the sample $\boldsymbol{u}(s)$ does not satisfy the bounds in (10) then the current iterate $\bar{\boldsymbol{x}}_p$ is updated so that the next iterate $\bar{\boldsymbol{x}}_{p+1}$ satisfies it using Equation (9). In the multi-level case, δ_q is chosen as follows

$$\begin{aligned} &\text{if } \sum_k \boldsymbol{v}(k,s) \bar{\boldsymbol{x}}_p(k) < \boldsymbol{u}_{low}(s) \Longrightarrow \delta_q = \boldsymbol{u}_{low}(s).\\ &\text{if } \sum_k \boldsymbol{v}(k,s) \bar{\boldsymbol{x}}_p(k) > \boldsymbol{u}_{high}(s) \Longrightarrow \delta_q = \boldsymbol{u}_{high}(s). \end{aligned}$$

This space-domain projection is different from the space-domain projection described in [2] in two aspects: (i) the convex sets that we define are different from the set defined in [2], and (ii) [2] is developed for a sigma-delta type error diffusion algorithm whereas our method is developed for the widely used Floyd-Steinberg error diffusion method. Due to the nature of our convex sets, $C_{1,s}$, the projection operation described in Eq. (9) is very simple to implement. This leads to a computationally more efficient reconstruction algorithm because, in each iteration of the POCS algorithm we do not update the entire image as in [2] but we modify only the pixels that do not meet the requirements.

2.2. Frequency-domain Projection

An important property of most natural images is smoothness compared to artificial images. This information can be imposed into the restoration process in the form of lowpass filtering. Therefore, the frequency-domain projection consists of bandlimiting the observed signal in some way. The simplest approach is lowpass filtering the image in order to remove the high-frequency components of the image, which contain mostly halftoning noise. For the frequency-domain projection, we either use a simple Gaussian lowpass filter $g(n_1, n_2) = k\ e^{-\frac{n_1^2+n_2^2}{2\sigma^2}}$, for $-3 \leq n_1, n_2 \leq 3$, where k is a scaling factor used to make the DC gain of the filter unity. The σ^2 controls the bandwidth of the lowpass filter. Or we use lowpass filters with passbands of $[-\pi/2,\ \pi/2] \times [-\pi/2,\ \pi/2]$, $[-2\pi/3,\ 2\pi/3] \times [-2\pi/3,\ 2\pi/3]$, or $[-3\pi/4,\ 3\pi/4] \times [-3\pi/4,\ 3\pi/4]$.

2.3. Space-scale Domain Projection

The edges in an image produce local WT extrema in the space-scale domain [9]. It is proved that the wavelet extrema information correspond to convex sets in $\mathcal{L}_2^2$ which is the set of square summable images [9, 10, 11]. Therefore, the edge information can be used in the reconstruction algorithm by properly defining a set corresponding to the significant local extrema in the wavelet domain. Let the set $\boldsymbol{C}_3$, contain all the images having the same significant WT local extrema as the original image. The key idea is to estimate the edges of the original image from the halftoned image by selecting the significant WT extrema of the halftoned image, and the restored image is forced to have the same extrema in the wavelet space-scale domain. This provides the sharpness to the restored image by protecting the significant high frequency components of the image, whereas a simple lowpass filtering characterized by set $\boldsymbol{C}_2$ will smooth out all of the sharp edges of the original image. The projection onto this set can be carried out as described in [10]. Another approach is to use the wavelet-based single step inverse halftoning method [5]. Although this method can not be considered as an orthogonal projection due to the cross-scale correlation operation, it is relatively easy to implement and can be incorporated to the iterative restoration procedure. In [5], important high frequency information describing the signal, particularly information in edge regions, are retained by choosing the WT extrema locations selectively from each subband resulting from the wavelet decomposition of the halftoned image. In our iterative restoration algorithm this method is used as an initial step.

3. SIMULATION RESULTS

To demonstrate the performance of our POCS-based inverse halftoning method, we present some simulation results with 512×512 Peppers and Zelda images. We compare the new method with some state-of-the-art inverse halftoning techniques in terms of their PSNRs. In the first group of simulations, we use space-domain and frequency-domain projections alternately. The first estimate of the contone image, $\boldsymbol{x}_1$ is obtained by lowpass filtering the input halftone image, $\boldsymbol{x}_0$ with $g(n_1, n_2)$. Then we perform our spatial projections. After that, we again use lowpass filtering, and go on in an alternating fashion. A section of the original 8 bpp Zelda image error-diffused to 1 bpp is shown in Figure 3. The initial estimate image with PSNR=32.85 dB, i.e. after the first frequency-domain projection, and the result of the two set of iterations with PSNR=33.37 dB are given in Figure 4, and Figure 5 respectively. The resulting image is quite sharp, and its visual quality is high. The details are restored while much of the halftoning noise existing in the first estimate is removed. The quality of the restoration of the detail regions can be observed around the eyes and mouth.

We compare our results with those in [2] in Table 1 for the Lena image. The PSNR improvement achieved by the proposed method is about 0.8 dB higher than the ones in [2], and the image quality is higher.

Apart from the binary error diffusion coding, we carried out simulation studies for images error-diffused to 2 bpp as shown in Figure 6 for the Zelda image. We use our method tailored for the multi-level case. The PSNR improvement over the initial estimate is about 0.6 dB with our POCS based method after two set of iterations, and our restoration results in a quite sharp, and faithful reproduction as can be seen in Figure 7 (PSNR=35.39 dB).

We can use wavelet-based space-scale domain projection in [5] as the initial estimate in our method. The resulting image after applying our method is shown in Figure 8 for the Peppers image (PSNR=30.90 dB). Even after a single set of iteration, i.e. by applying our space-domain projections following wavelet-based projection in [5], our space-domain projections achieves around 0.5 dB improvement over the initial estimate.

Comparison of the POCS-based method with other existing methods are given in Table 2 for the Peppers and Lena images. Our method results in a higher PSNR than the other two methods in [1, 5] for both of the images.

Halftoned color images can also be restored using the proposed method. Our spatial projection for the multilevel halftoning case can be applied to color images where each color pixel takes values from the color palette of limited size such as 8, 16, or more. By using the constraint in (6) for each color pixel, we find the two closest colors from the palette, and we project each color vector to the closest color by simply scaling its each color component red, green, and blue. As a second method to color image inverse halftoning, we do inverse halftoning only on the luminance component of the color image. Then the inverse halftoned image is obtained together with the lowpass filtered versions of the chrominance components.

Some sample simulation results of the work presented in this paper can be viewed at http://www4.ncsu.edu/∼gbozkur.

4. CONCLUSIONS

In this paper, a new set theoretic inverse halftoning method to restore the continuous tone images from their halftone versions is introduced. Prior information about the error diffusion process and the original image is modeled as convex sets. The original image is assumed to be in the intersection of these convex sets onto which successive projections are made in our iterative restoration algorithm. The iterates converge to a feasible solution. It is experimentally observed that the restored image has a higher PSNR than the other methods existing in the literature.

5. REFERENCES

[1] P.W. Wong. Inverse halftoning and kernel estimation for error diffusion. *IEEE Trans. Image Process.*, 4(4):486–498, 1995.

[2] S. Hein and A. Zakhor. Halftone to continous-tone conversion of error-diffusion coded images. *IEEE Trans. Image Process.*, 4(2):208–215, 1995.

[3] R.L. Stevenson. Inverse halftoning via map estimation. *IEEE Trans. Image Process.*, 6(4):574–583, 1997.

[4] M. Analoui and J. Allebach. New results on reconstruction of continous-tone from halftone. In *Proc. IEEE Int. Conf. Acoust. Speech Signal Process.*, pages 313–316, 1992.

[5] Z. Xiong, M.T. Orchard, and K. Ramchandran. Inverse halftoning using wavelets. In *Proc. IEEE Int. Conf. on Image Processing*, pages 569–572, 1996.

[6] G. Bozkurt. Novel methods in image halftoning. Master's thesis, Bilkent University, 1998.

[7] P.L. Combettes. The foundations of set theoretic estimation. *Proc. IEEE*, 81(2):182–208, 1993.

[8] J.S. Lim. *Two-dimensional Signal and Image Processing*. Prentice Hall, New Jersey, 1990.

[9] S. Mallat and S. Zhong. Characterization of signals from multiscale edges. *IEEE Trans. Pattern Analysis, and Machine Intelligence*, 14(7):710–732, 1992.

[10] A.E. Çetin and R. Ansari. Signal recovery from wavelet transform maxima. *IEEE Trans. Signal Process.*, 42(1):194–196, 1994.

[11] A.H. Tewfik and H. Zou. Completeness of arbitrarily sampled discrete time wavelet transforms. *IEEE Trans. Signal Process.*, 43(11):2570–2581, 1995.

[2] (GLPF)	[2] (SVD)	Our Method (GLPF, LPF)
29.4	30.4	31.23

Table 1: Comparison of PSNRs (dB) for the inverse halftoning methods in [2], and our method for the Lena Image. The (GLPF, LPF, SVD) denotes the type of frequency-domain projection.

	Method[1]	Method [5]	Our Method
Lena (PSNR)	32.00	31.67	32.17
Peppers (PSNR)	30.30	30.69	30.90

Table 2: Comparison of inverse halftoning methods. All methods assume the error diffusion kernel is known.

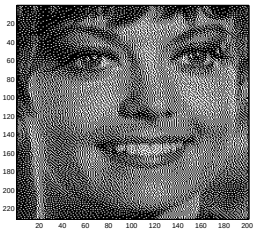

Figure 3: Zelda image error-diffused to 1 bbp.

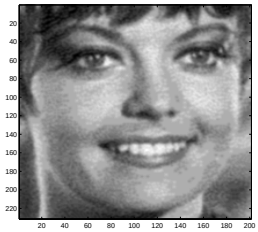

Figure 4: First estimate (PSNR=32.85 dB).

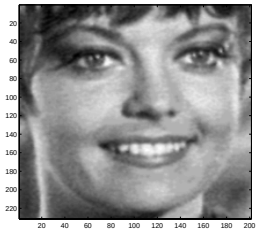

Figure 5: Restored Zelda image (PSNR=33.37 dB).

Figure 6: Zelda image error-diffused to 2 bbp.

Figure 7: Restored Zelda image (PSNR=35.39 dB).

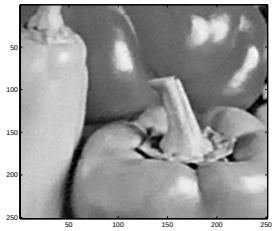

Figure 8: Restored peppers image (PSNR=30.90 dB).